Lithium-Ion Batteries

DOI: 10.1002/ange.201404510

A First-Cycle Coulombic Efficiency Higher than 100 % Observed for a Li_2MO_3 (M = Mo or Ru) Electrode**

*Jihyun Jang, Youngjin Kim, Oh B. Chae, Taeho Yoon, Sang-Mo Kim, Hyun-seung Kim, Hosang Park, Ji Heon Ryu, and Seung M. Oh**

Abstract: *The lithiation/de-lithiation behavior of a ternary oxide (Li_2MO_3, where M = Mo or Ru) is examined. In the first lithiation, the metal oxide (MO_2) component in Li_2MO_3 is lithiated by a conversion reaction to generate nano-sized metal (M) particles and two equivalents of Li_2O. As a result, one idling Li_2O equivalent is generated from Li_2MO_3. In the de-lithiation period, three equivalents of Li_2O react with M to generate MO_3. The first-cycle Coulombic efficiency is theoretically 150 % since the initial Li_2MO_3 takes four Li^+ ions and four electrons per formula unit, whereas the M component is oxidized to MO_3 by releasing six Li^+ ions and six electrons. In practice, the first-cycle Coulombic efficiency is less than 150 % owing to an irreversible charge consumption for electrolyte decomposition. The as-generated MO_3 is lithiated/de-lithiated from the second cycle with excellent cycle performance and rate capability.*

The demand for large-capacity lithium-ion batteries (LIBs) has been increasing for applications in electric vehicles and energy-storage systems.[1] Graphite is the most commonly used negative electrode in present-day LIBs.[2] Owing to the limited capacity of this carbon-based material, alternative electrode materials have been developed.[3] One example is the metal oxides that can be lithiated by a conversion reaction.[4] In that reaction, the metal–oxygen bonds are broken and the metal (M) ions are reduced to their elemental states by taking injected electrons, while the co-injected Li ions are converted into Li_2O as in Equation (1).

$$MO_2 + 4\,Li^+ + 4\,e \rightarrow M + 2\,Li_2O \quad (1)$$

It is generally accepted that nano-sized metal particles are embedded into the Li_2O matrix. Unexpectedly, the reverse reaction is also allowed since nano-sized metal particles can enhance the electrochemical activity related to the decomposition of Li_2O and metal–oxygen bond formation. This feature has been ascribed to the large contact area between the metal particles and the Li_2O matrix.[5]

The concept investigated in this study is related to the high level of reaction activity between metal and Li_2O.[6] Namely, if Li_2O forms Li_2MO_3 by a combination with metal oxide (MO_2) component, the MO_2 is lithiated to generate a mixture of M and Li_2O nano-particles, while the Li_2O component in the initial Li_2MO_3 phase is idle (a spectator), as in Equation (2)

$$Li_2MO_3 + 4\,Li^+ + 4\,e \rightarrow M + 2\,Li_2O + Li_2O \quad (2)$$

As a result, the M component establishes an intimate contact with three equivalents of Li_2O (two by the lithiation reaction and one idle). If three equivalents of Li_2O react with M, then MO_3 can be generated as in Equation (3).

$$M + 3\,Li_2O \rightarrow MO_3 + 6\,Li^+ + 6\,e \quad (3)$$

For this reaction to be practicable, two conditions should be met. First, the contact area between M and Li_2O should be large enough for all of the available M and Li_2O to react to produce MO_3. It is very likely that this condition is met since both are generated from the molecular-level mixture (Li_2MO_3). Second, the M component should be oxidized up to M^{6+} within the working potential range of the negative electrode. In this study, Mo and Ru are selected as the M component since Mo^{6+} and Ru^{6+} compounds can be prepared electrochemically. A highly crystalline Li_2MO_3 (hereafter M = Mo or Ru) phase is prepared and its lithiation/de-lithiation behavior is examined. If a Li_2MO_3 electrode is lithiated/de-lithiated according to the above scheme, its theoretical first-cycle Coulombic efficiency is 150 % because the initial Li_2MO_3 phase is lithiated by taking four Li^+ ions and four electrons, and de-lithiated by releasing six Li^+ ions and six electrons per formula unit. The prime concern in this study is to confirm whether the Li_2MO_3 electrode can provide a Coulombic efficiency of 150 % in the first-cycle lithiation/de-lithiation cycle and to examine the electrode performance of MO_3 generated by Equation (3).

Figure 1 presents the voltage profiles of a $Li\,|\,Li_2MoO_3$ cell and those obtained from $Li\,|\,MoO_2$ and $Li\,|\,MoO_3$ cells for comparison. The MoO_2 electrode (Figure 1a) is lithiated by an insertion reaction near 1.5 V (vs Li/Li^+), which is followed by a conversion reaction at constant voltage step (0.0 V)in the first cycle.[7] Similarly, the MoO_3 electrode (Figure 1b) is lithiated by an insertion reaction near 2.5 V followed by a conversion reaction near 0.5 V.[8] The difference in the conversion reaction potential between MoO_2 and MoO_3 is the result of the difference in bond strengths (bond dissociation

[*] J. Jang, Y. Kim, O. B. Chae, T. Yoon, S.-M. Kim, H. S. Kim, H. Park, Prof. S. M. Oh
Department of Chemical and Biological Engineering
Seoul National University
Seoul 151-744 (Korea)
E-mail: seungoh@snu.ac.kr
Prof. J. H. Ryu
Graduated School of Knowledge-based Technology and Energy
Korea Polytechnic University, Siheung-si (Korea)

[**] This work was supported by MEST through NRF-2010-C1AAA001-2010-0029065.

Supporting information for this article is available on the WWW under http://dx.doi.org/10.1002/anie.201404510.

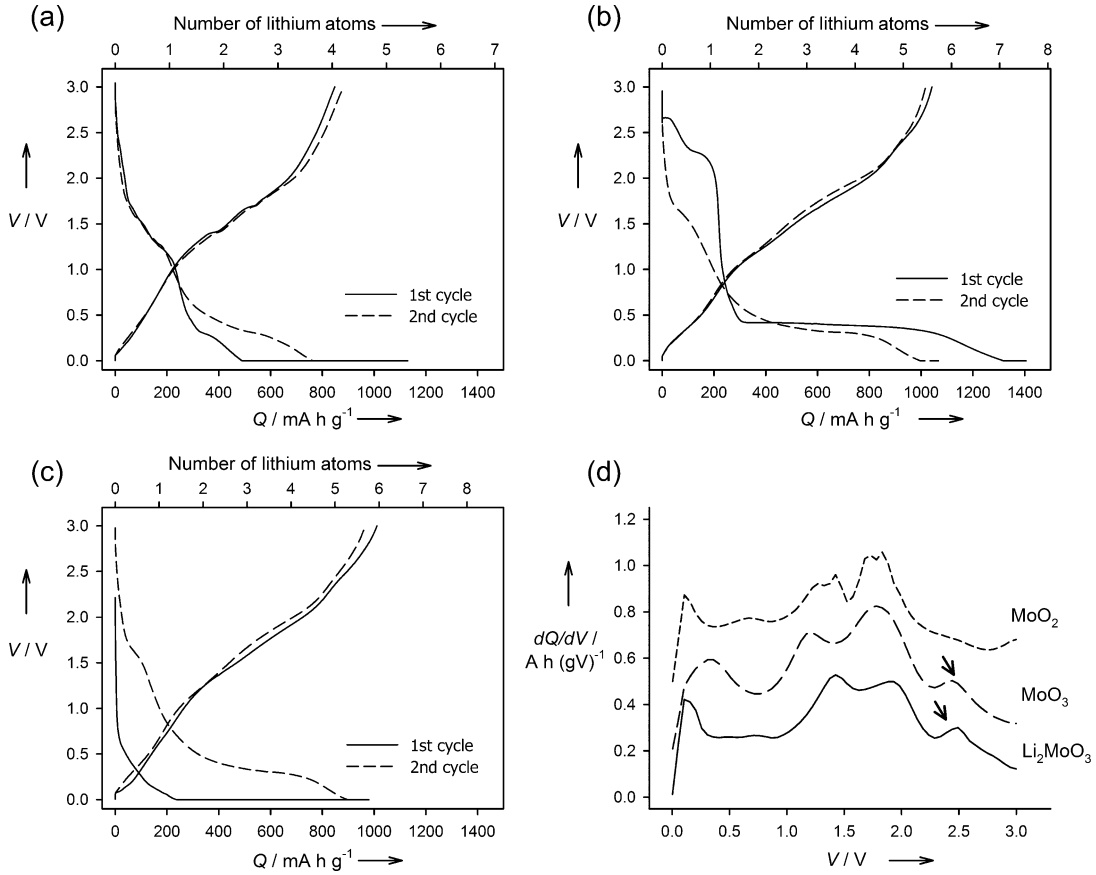

Figure 1. First- and second-cycle lithiation/de-lithiation voltage profiles of a) Li | MoO_2, b) Li | MoO_3, c) Li | Li_2MoO_3 cells, and d) differential first-cycle de-lithiation capacity profiles for MoO_2, MoO_3, and Li_2MoO_3 electrodes. Voltage is measured versus Li/Li^+. See text for details.

energy of Mo–O in MoO_3 and MoO_2 are 565 and 678 kJ mol^{-1}, respectively).[9] The Li_2MoO_3 electrode (Figure 1 c) shows a voltage plateau at constant voltage step 0.0 V) in the first cycle, indicative of a conversion reaction occurring in this tertiary oxide. The X-ray diffraction (XRD) analysis illustrates that the highly crystalline Li_2MoO_3 structure collapses to an amorphous and/or nano-crystalline phase after lithiation (Supporting Information, Figure S1-a). The presence of a conversion reaction in the voltage plateau region (0.0 V) can be ascertained from the bell-shape current behavior (Figure S1-b), which is a signature of two-phase reactions.[10] Note that the bond breaking conversion-type lithiation is a two-phase reaction. In addition, through the Mo K-edge X-ray absorption near-edge structure (XANES) spectra for lithiated electrode (Figure S2), it can be deduced that Li_2MoO_3 electrode is lithiated by conversion reaction to generate metallic Mo.

The de-lithiation capacity of MoO_2 and MoO_3 electrodes is well-matched with what is expected from a conversion reaction. The MoO_2 is de-lithiated in the first cycle by releasing four Li^+ ions and four electrons, whereas the number of released Li^+ ions and electrons is six for the MoO_3. This indicates that metallic Mo is generated from both MoO_2 and MoO_3 electrodes upon lithiation, and the as-generated Mo metal is oxidized back to MoO_2 and MoO_3, respectively. In the case of the Li_2MoO_3, however, the de-lithiation capacity is six Li^+ ions and six electrons in the first cycle (Figure 1 c), strongly indicating that the metallic Mo generated by a conversion reaction of the Li_2MoO_3 is oxidized up to Mo^{6+} (MoO_3) in the forthcoming de-lithiation period.

The extension of oxidation up to Mo^{6+} is ascertained from the differential first-cycle de-lithiation capacity (dQ/dV) profiles shown in Figure 1 d. As shown, the Mo metal that is generated by the conversion reaction of MoO_2 is oxidized back to MoO_2 over the potential range of 0.0 to 2.0 V upon de-lithiation. The potential range, where the Mo metal generated by the conversion reaction of MoO_3 is oxidized back to MoO_3, extends up to 2.5 V. A peak at 2.5 V, which is absent for MoO_2 electrode, appears in the MoO_3 electrode (arrow in Figure 1 d). It is thus very likely that oxidation from Mo^{4+} to Mo^{6+} takes place near 2.5 V. Another feature apparent in Figure 1 d is that the peak at 2.5 V for the MoO_3 electrode also appears in the dQ/dV profile for the Li_2MoO_3 electrode, strongly suggesting that the metallic Mo is oxidized up to M^{6+} (MoO_3) in the de-lithiation period. The lithiation and de-lithiation process for Li_2MoO_3 is schematically illustrated in Scheme S1 in the Supporting Information.

The Mo valence change from Mo^{4+} in the initial Li_2MoO_3 phase to Mo^{6+} is confirmed by analyzing the Mo K-edge XANES spectra, in which a pre-edge appears, of which the intensity is deeply associated with the local symmetry of Mo.[11] The intensity of the pre-edge peak is very low for

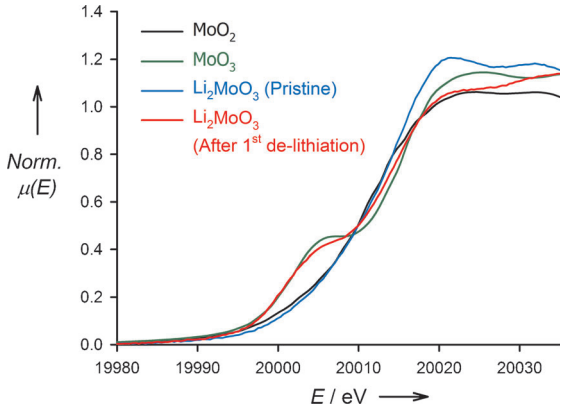

Figure 2. The normalized Mo K-edge XANES spectra for the Li_2MoO_3 electrode. Note that the pristine Li_2MoO_3 electrode does not show a pre-edge peak like that shown by the MoO_2 electrode. However, the Li_2MoO_3 electrode does show a pre-edge peak after the first charge/discharge cycle.

MoO_2 since the Mo^{4+} ions are placed in a rather symmetric site (a slightly distorted MoO_6 octahedron; Figure 2).[12] In contrast, the pre-edge peak is stronger in MoO_3 because the local symmetry of the MoO_6 octahedron is low due to four shorter Mo–O bonds and two longer Mo-O bonds.[13] The pristine Li_2MoO_3 electrode does not show a pre-edge like that in MoO_2 because the Mo^{4+} ions in Li_2MoO_3 are located in the ordinary octahedral sites.[14] After the first-cycle de-lithiation, however, a pre-edge like that in MoO_3 develops in the Li_2MoO_3 electrode, implying that the Mo valence is Mo^{6+} in the de-lithiated Li_2MoO_3 electrode.

Theoretically, the first-cycle Coulombic efficiency of the Li_2MoO_3 electrode should be 150% since this electrode accepts four Li^+ and four electrons in lithiation and releases six Li^+ ions and six electrons per formula unit. However, the experimentally observed value is 106% (Table 1). This discrepancy is due to an irreversible charge consumption associated with electrolyte decomposition. That is, the first-cycle lithiation capacity is larger than four Li^+ ions and four electrons per formula unit because of irreversible charge consumption. The MoO_2 and MoO_3 electrodes also show larger lithiation capacity than their theoretical values for the same reason, resulting in their low first-cycle Coulombic efficiency.

The second-cycle lithiation voltage profile of the Li | Li_2MoO_3 cell is markedly different from that observed in the first-cycle lithiation (Figure 1c). Rather, it is quite similar to that observed in the second cycle of the MoO_3 electrode (dashed line in Figure 1b). In the MoO_3 electrode, the crystalline phase is converted into amorphous and/or nano-sized MoO_3 after a charge/discharge cycling.[8b] Hence, the lithiation voltage profile obtained in the second cycle is the lithiation profile for amorphous and/or nano-sized MoO_3. The similarities in the second-cycle lithiation profiles of the MoO_3 and Li_2MoO_3 electrodes illustrate that the crystalline Li_2MoO_3 phase is also converted into amorphous and/or nano-sized MoO_3 after the first charge/discharge cycling, and it is charged/discharged from the second cycle. The cycle performance and rate capability of amorphous and/or nano-sized MoO_3, which is derived from Li_2MoO_3, are presented in Figure 3. Surprisingly, the results show a very stable cycle performance without serious capacity loss. The de-lithiation capacity in the 50th cycle amounts to 900 mA h g^{-1}, which corresponds to a release of 5.3 Li^+ ions and 5.3 electrons per formula unit. The rate performance is also excellent with a de-lithiation capacity of 600 mA h g^{-1} at a current density of 2000 mA g^{-1}.

Two additional experiments elucidate further the suggested mechanism. The first test is of a physical mixture of MoO_2 and Li_2O. The MoO_2/Li_2O mixture electrode releases five Li^+ ions and five electrons per formula unit. The dQ/dV peak near 2.5 V is also observed in this electrode and the first-cycle Coulombic efficiency is 87% (Figure S3). This efficiency is greater than that observed with the MoO_2 electrode, but is less than that for the Li_2MoO_3 electrode. The latter difference must be due to the smaller Mo/Li_2O contact area in the physically mixed sample. The results, however, demonstrate that the added Li_2O can participate in a bond-forming

Table 1: The first-cycle lithiation, de-lithiation capacity, and Coulombic efficiency for MoO_2, MoO_3, and Li_2MoO_3 electrodes.

Electrode	First-cycle Lithiation capacity [mA h g^{-1}]	First-cycle De-lithiation capacity [mA h g^{-1}]	First-cycle Coulombic efficiency [%]
MoO_2	1130	848	75.0
MoO_3	1405	1042	74.2
Li_2MoO_3	954	1011	106.0

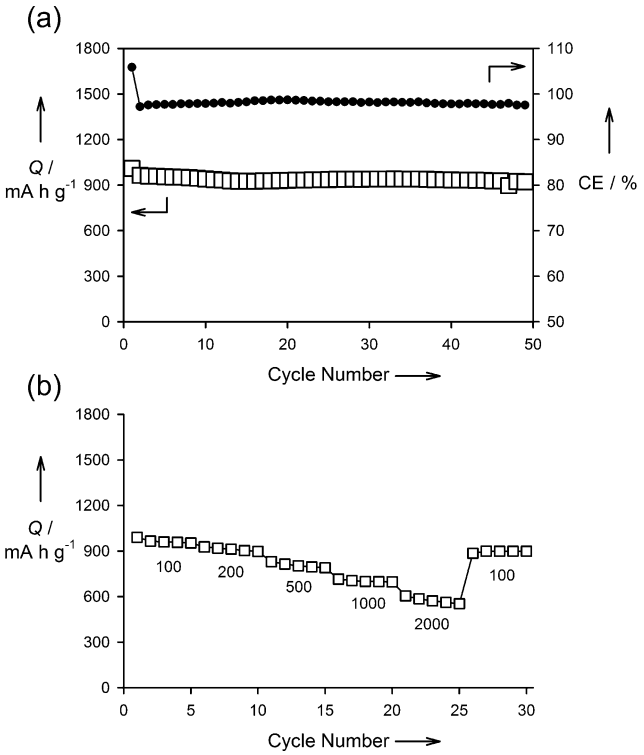

Figure 3. a) The cycle performance and Coulombic efficiency (CE), and b) rate capability of the Li | Li_2MoO_3 cell. The current density (in mA g^{-1}) is indicated below the data points.

reaction if it makes intimate contact with metal components that can be oxidized to higher oxidation states. This feature is investigated further by assessing the results obtained from a Li_2RuO_3 electrode. Note that Ru can be oxidized up to Ru^{6+} state at under 4.0 V.[15] As shown in Figure S4, the Li_2RuO_3 electrode has a high Coulombic efficiency (120%) in the first cycle, implying that Li_2RuO_3 is converted into a mixture of metallic Ru and three equivalents of Li_2O by taking four Li^+ ions and four electrons, and the metallic Ru is oxidized to RuO_3 by releasing six Li^+ ions and six electrons in the forthcoming de-lithiation period. The high Coulombic efficiency of the Li_2RuO_3 electrode, compared to that of the Li_2MoO_3 electrode is ascribed to the re-oxidation of solid electrolyte interphase films at over 3 V.[16]

Finally, to utilize the high first-cycle Coulombic efficiency of Li_2MoO_3, it is blended with a SiO electrode that normally has poor first-cycle Coulombic efficiency. The Li_2MoO_3/SiO blended electrode has a markedly higher first-cycle Coulombic efficiency (77.4%) than that of a pure SiO electrode (54.7%; Figure S5, Table S1). The experimental value is higher than the calculated one (69%), because Mo metal remained at the potential range where the de-alloying of Li–Si phase takes place (near 0.4 V) facilitates the de-lithiation of Li–Si alloy. (Figure S6).

In conclusion, the MO_2 component in a Li_2MO_3 (M = Mo or Ru) is lithiated by a conversion reaction to generate a mixture of M and Li_2O. An idle Li_2O is isolated during this reaction. The idle Li_2O participates in the de-lithiation reaction to produce MO_3. As a result, the theoretical first-cycle Coulombic efficiency is 150%. It can be generalized that nano-sized metallic components, which are generated by a conversion reaction, can react with Li_2O regardless of whether the Li_2O is provided by a molecular-level or physical mixture. Furthermore, if such metallic components can be oxidized to higher valence states, the de-lithiation capacity can exceed the lithiation capacity to give a Coulombic efficiency higher than 100%.

Received: April 21, 2014
Published online: August 11, 2014

Keywords: Coulombic efficiency · electrochemistry · energy conversion · lithium-ion batteries · metal oxide electrode

[1] a) J. M. Tarascon, M. Armand, *Nature* **2001**, *414*, 359 – 367; b) T.-H. Kim, J.-S. Park, S. K. Chang, S. Choi, J. H. Ryu, H.-K. Song, *Adv. Energy Mater.* **2012**, *2*, 860 – 872.
[2] J. R. Dahn, T. Zheng, Y. Liu, J. S. Xue, *Science* **1995**, *270*, 590 – 593.
[3] a) J. Cabana, L. Monconduit, D. Larcher, M. R. Palacin, *Adv. Mater.* **2010**, *22*, E170 – 192; b) M. V. Reddy, G. V. Subba Rao, B. V. R. Chowdari, *Chem. Rev.* **2013**, *113*, 5364 – 5457.
[4] a) C. H. Kim, Y. S. Jung, K. T. Lee, J. H. Ku, S. M. Oh, *Electrochim. Acta* **2009**, *54*, 4371 – 4377; b) Y. Shi, B. Guo, S. A. Corr, Q. Shi, Y.-S. Hu, K. R. Heier, L. Chen, R. Seshadri, G. D. Stucky, *Nano Lett.* **2009**, *9*, 4215 – 4220; c) O. B. Chae, S. Park, J. H. Ryu, S. M. Oh, *J. Electrochem. Soc.* **2012**, *160*, A11 – A14; d) J. Wang, N. Yang, H. Tang, Z. Dong, Q. Jin, M. Yang, D. Kisailus, H. Zhao, Z. Tang, D. Wang, *Angew. Chem.* **2013**, *125*, 6545 – 6548; *Angew. Chem. Int. Ed.* **2013**, *52*, 6417 – 6420.
[5] a) P. Poizot, S. Laruelle, S. Grugeon, L. Dupont, J. M. Tarascon, *Nature* **2000**, *407*, 496 – 499; b) P. Poizot, S. Laruelle, S. Grugeon, J.-M. Tarascon, *J. Electrochem. Soc.* **2002**, *149*, A1212.
[6] Y. Yu, C. H. Chen, J. L. Shui, S. Xie, *Angew. Chem.* **2005**, *117*, 7247 – 7251; *Angew. Chem. Int. Ed.* **2005**, *44*, 7085 – 7089.
[7] a) J. H. Ku, Y. S. Jung, K. T. Lee, C. H. Kim, S. M. Oh, *J. Electrochem. Soc.* **2009**, *156*, A688 – A693; b) B. Guo, X. Fang, B. Li, Y. Shi, C. Ouyang, Y.-S. Hu, Z. Wang, G. D. Stucky, L. Chen, *Chem. Mater.* **2011**, *24*, 457 – 463.
[8] a) F. Leroux, L. F. Nazar, *Solid State Ionics* **2000**, *133*, 37 – 50; b) Y. S. Jung, S. Lee, D. Ahn, A. C. Dillon, S.-H. Lee, *J. Power Sources* **2009**, *188*, 286 – 291.
[9] B. d. Darwent, National Standard Reference Data Series: National Bureau of Standard No. 31, Washington **1970**.
[10] a) C. Wan Park, S.-H. Yoon, S. I. Lee, S. M. Oh, *Carbon* **2000**, *38*, 995 – 1001; b) X. Ma, H. Chen, G. Ceder, *J. Electrochem. Soc.* **2011**, *158*, A1307.
[11] N. S. Chiu, S. H. Bauer, M. F. L. Johnson, *J. Catal.* **1984**, *89*, 226 – 243.
[12] a) B. G. Brandt, A. C. Skapski, *Acta Chem. Scand.* **1967**, *21*, 661 – 672; b) J. R. Dahn, W. R. McKinnon, *Solid State Ionics* **1987**, *23*, 1 – 7.
[13] a) D. Lützenkirchen-Hecht, R. Frahm, *J. Phys. Chem. B* **2001**, *105*, 9988 – 9993; b) A. Tougerti, E. Berrier, A.-S. Mamede, C. La Fontaine, V. Briois, Y. Joly, E. Payen, J.-F. Paul, S. Cristol, *Angew. Chem.* **2013**, *125*, 6568 – 6572; *Angew. Chem. Int. Ed.* **2013**, *52*, 6440 – 6444.
[14] S. J. Hibble, I. D. Fawcett, *Inorg. Chem.* **1995**, *34*, 500 – 508.
[15] B. J. Hornstein, D. M. Dattelbaum, J. R. Schoonover, T. J. Meyer, *Inorg. Chem.* **2007**, *46*, 8139 – 8145.
[16] P. Balaya, H. Li, L. Kienle, J. Maier, *Adv. Funct. Mater.* **2003**, *13*, 621 – 625.

